were recorded with a low modulation amplitude (5×10^{-2} G). Knowing the total anion radical concentration and the ratio of the two concentrations gives us the concentration of both anion radical species. Sensitivity bias between the two cavities was corrected for by carrying out comparisons of doubly integrated spectra of identical DPPH samples in each of the cavities.

ESR and/or NMR samples were sealed from the all-glass apparatus under high vacuum. Weighed portions of the salts were placed directly in the ESR or NMR tubes prior to initiation of the experiment. In this way, the salts could be kept under high vacuum for several hours prior to the addition of the solvent. This technique also allowed us to take ESR and NMR samples of the same solution with no salt present and with various concentrations of the salt added. The concentrations of added KI and NaI varied from 0.01 to 0.1 M.

Neutral [8]annulene was added to the anion radical solutions via break seals. The amount of metal used in the reduction was varied so as to keep the anion radical concentration constant.

NMR spectra were recorded on a Perkin-Elmer 60-MHz spectrometer. The HMPA was purified as previously described[12] and was distilled directly into the apparatus where the reductions were carried out. All of the reductions took place on a freshly distilled sodium surface under high vacuum.

Registry No. $[8]^{-\cdot}$, 34510-85-5.

Energetics and Hydration Structures of a Solvated Gramicidin A Transmembrane Channel for K^+ and Na^+ Cations

Kwang S. Kim and E. Clementi*

Contribution from IBM Corporation, Department 48B, Kingston, New York 12401.
Received September 26, 1984

Abstract: This paper analyzes the strength of the interaction energies of the K^+ and Na^+ ions with GA along a transmembrane channel axis. The detailed hydration structures in the channel in the presence of these ions are described from Monte Carlo simulations. The nine water molecules inside the channel strongly hydrate the GA carbonyl oxygens. The interaction energy of these water molecules with GA is much larger than that with water or an ion. This fact, combined with the small cross sections of the GA channel, suggests that an ion will push a column of water ahead of it in order to pass through the channel. The energetics of solvation and hydration are also analyzed. For a linear strand of water molecules in the channel, the contribution of the solvation energy from higher solvation shells decreases rapidly because we included bulklike water outside the channel mouth. Within a rigid GA frame, this work also indicates that inside the channel the Na^+ ion moves along a helical path in between two layers of GA backbone atoms, while the K^+ ion moves roughly linearly along the cylindrical axis of the channel.

I. Introduction

The ion selectivity of a biological membrane plays an important role in many biomechanisms, At present, the gramicidin channel is the only ion-selective transmembrane with a well-characterized structure. This single transmembrane structure is impermeable to anions and divalent cations. However, it exhibits selectivity among monovalent cations with permeability ratios (with respect to sodium) of $H^+(150) > NH_4^+(8.9) > Cs^+(5.8) > Rb^+(5.5) > K^+(3.9) > Na^+(1.0) > Li^+(0.33)$, as earlier reported by Myers and Haydon.[1] Interest in the gramicidin channel has been enhanced due to its complex conductance properties, such as ion selectivity, voltage and concentration dependence of permeability ratios, etc., as the number and scope of studies has increased greatly in recent years. For recent reviews, see Urry,[2] Ovchinnikov,[3] Eisenman and Horn,[4] and Andersen.[5]

Since GA has a relatively simple and well-defined structure, there is a wealth of experimental data. Many conformational studies,[6] simple electrostatic model studies,[7] and simple molecular dynamics (MD) studies[8] have also been reported, Although some of these reports show reasonable agreement with experiment, some of the models used are still too simple to be reliable, or the reliability of some potentials used is questionable.

Wilson et al.[9] recently studied the interaction of GA with cations and a few water molecules by using MD techniques. Although their model included intramolecular interaction energies of GA, it still used vacuum instead of bulk water outside the channel; thus, energy profiles cannot be easily obtained owing to the neglect of solvation effects by bulk water and the temperature fluctuations in MD techniques (which are caused by the small number of water molecules and one cation), In particular, as noted in their paper, uncertainties in the potentials used were one of the shortcomings of the study. Other recent theoretical studies of energy profiles of Na^+ interacting with GA have been reported by Pullman et al.[10] In their papers, however, solvation effects and temperature and statistical effects were not considered. Furthermore, the binding energy of Na^+ and GA was obtained by using parameters which were fitted to mimic the results of ab initio calculations on small systems.

To lessen potential problems, we recently reported the ab initio atom-atom pair interaction energies of potassium,[11] sodium,[12] and

(1) Myers, V. B.; Haydon, D. A. *Biochim. Biophys. Acta* **1972**, *274*, 313-322.

(2) (a) Urry, D. W. in "Membranes and Transport"; Martonosi, A. N., Ed.; Plenum Press: New York, 1982; Vol. 2, pp 285-294. (b) Urry, D. W. *Top. Curr. Chem.*, in press.

(3) (a) Arseniev, A. S.; Bystrov, V. F.; Ivanov, V. T.; Ovchinnikov, Y. A. *Fed. Eur. Biochem. Soc.* **1984**, *165*, 51-56. (b) Ovchinnikov, Y. A.; Ivanov, V. T. In "Conformation in Biology"; Srinivasan, R., Sarma, R. H., Eds.; Adenine Press: New York, 1983; pp 155-174.

(4) Eisenman, G.; Horn, R. *J. Membr. Biol.* **1983**, *76*, 197-225.

(5) Andersen, C. S. *Annu. Rev. Physiol.* **1984**, *46*, 531-548.

(6) (a) Fraga, S.; Nilar, S. H. M. *Can. J. Biochem. Cell Biol.* **1983**, *61*, 856-859. (b) Venkatachalam, C. M.; Urry, D. W. *J. Comput. Chem.* **1984**, *5*, 64-71. (c) Ramachandran, G. N.; Urry, D. W. *J. Comput. Chem.* **1984**, *5*, 64-71. (c) Ramachandran, G. N.; Ramachandran, R. *Ind. J. Biochem. Biophys.* **1972**, *9*, 1-11. (d) Popov, E. M.; Lipkind, G. M. *Molec. Biol. (Engl. Transl.)* **1979**, *13*, 363-376. (e) Venkatram-Prasad, B. V.; Chandrasekaran, R. *Int. J. Peptide Protein Res.* **1977**, *10*, 129-138.

(7) (a) Parseigan, V. A. *Ann. N.Y. Acad. Sci.* **1975**, *264*, 161-174. (b) Levitt, D. G. *Biophys. J.* **1978**, *22*, 209-219. (c) Jordan, P. C. *Biophys. Chem.* **1981**, *13*, 203-212. (d) Jordan, P. C. *Biophys. J.* **1984**, *45*, 1091-1100.

(8) (a) Brickmann, J.; Fischer, W. *Biophys. Chem.* **1983**, *17*, 245-258. (b) Fischer, W.; Brickmann, J.; Lauger, P. *Biophys. Chem.* **1981**, *13*, 105-116. (c) Fischer, W.; Brickmann, J. Paper presented at the Bioelectrochemistry and Bioenergetics Proceedings of the International Meeting, Physical Chemistry of Transmembrane Ion Motions, Paris, 1982. (d) Schroder, H.; Brickmann, J.; Fisher, W. *Mol. Phys.* **1983**, *11*, 1-11.

(9) Mackay, D.J.; Berens, P. H.; Wilson, K. R.; Hagler, A. T. *Biophys. J.* **1984**, *46*, 229-248.

(10) (a) Pullman, A.; Etchebest, C. *Fed. Eur. Biochem. Soc.* **1983**, *163*, 199-202. (b) Etchebest, C.; Pullman, A. *Fed. Eur. Biochem. Soc.* **1984**, *170*, 191-195. (c) Etchebest, C.; Ranganathan, S.; Pullman, A. *Fed. Eur. Biochem. Soc.* **1984**, *173*, 301-306.

(11) Kim, K. S.; Vercauteren, D. P.; Welti, M.; Chin, S.; Clementi, E. *Biophys. J.* **1985**, *47*, 327-335.

(12) Kim, K. S.; Vercauteren, D. P.; Welti, M.; Fornili, S. L.; Clementi, E. unpublished results.

0002-7863/85/1507-5504$01.50/0

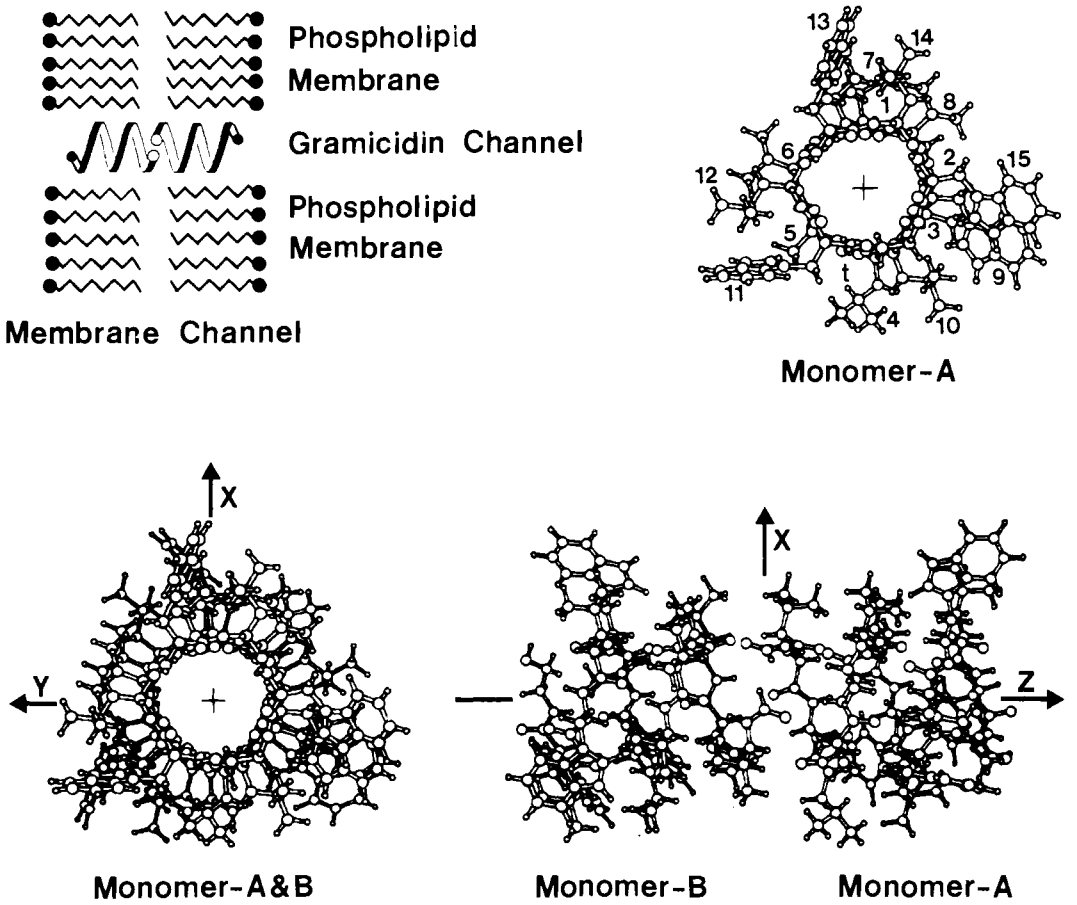

Figure 1. Features of a GA membrane channel. Top-left: schematic representation of a membrane channel. Top-right: projection of a GA monomer onto X–Y plane with labels for the 15 residues. Bottom: projections of a GA channel (GA dimer) onto X–Y plane (left) and X–Z plane (right).

water[13] with GA, modeled according to Urry's atomic coordinates,[14] We also reported preliminary MC simulation results[11,12] with these interaction energies, MCY potential[15] for water–water interactions, and the refitted and simplified 6-12-1 potential[13] of Kistenmacher et al,[16] for water–cation interaction energies. In this paper, we analyze strength of cation–channel interaction energies along a GA channel axis and compare the difference between K^+ and Na^+. Detailed analyses of hydration structure in the channel in the presence of K^+ and Na^+ cations are also described.

One of the shortcomings of our model is to assume GA to be rigid. We did not allow intramolecular interaction in GA. Although ref 9 shows that the carbonyls librate strongly inside the channel, the potentials used did not consider the anharmonicity of the potentials due to the change of the conformations of amide bondings and carbonyl librations. We note that GA structural changes are strongly anharmonic.[17] On the other hand, the selection of only one GA configuration will impose limitations on our findings.

II. Interaction Energetics of K^+ and Na^+ Ions with GA

Before discussing the interaction energetics, we first examine the structure of GA in detail. The primary structure of gramicidin A (GA) was characterized by Sarges and Witkop[18] to be HCO-L-Val^1-Gly^2-L-Ala^3-D-Leu^4-L-Ala^5-D-Val^6-L-Val^7-D-Val^8-L-Trp^9-D-Leu^{10}-L-Trp^{11}-D-Leu^{12}-L-Trp^{13}-D-Leu^{14}-L-Trp^{15}-$NHCH_2CH_2OH$. In this paper, we use the GA coordinates provided by Urry.[14] Figure 1 shows a GA membrane channel. At the top left of the figure, the GA channel consisting of a GA dimer is surrounded by the phospholipid membrane. At the top right of the figure, a GA monomer is projected onto the X–Y plane (the Z axis lies along the axis of the channel), where the 15 amino acid residues of GA are explicitly labeled. In the bottom-right inset, a GA dimer is projected onto the X–Z plane. The bottom-left inset (a projection onto the X–Y plane) clearly shows the cavity that makes up the channel along with the various amino acid residues attached to the two monomer backbones.

Figure 2 shows cylindrical maps of GA and their R–Z projections. The reference frame is the cylindrical surface with a radius of R = 3.5 Å. The gramicidin transmembrane channel is a dimer. Each monomer is a β-helix in which there are 6.3 residues per turn and in which the peptide C–O moieties alternately point toward the carbonyl end (L residues) and toward the amino end (D residues). The A and B monomers are related by a 2-fold axis. The sense of the GA helix is left-handed.

Figure 2a shows all the atoms of GA, while Figure 2b shows only the backbone atoms in order to represent key structures. The right-most figure in each inset is the R–Z projection of the cylindrical map. The R–Z projection in inset b includes only carbonyl atoms in order to show where the carbonyl oxygens are located. The atoms of the backbone are close to the Z axis, lying between R = 2.9 and 4.0 Å, while the atoms of the residues lie at $R >$ 5.1 Å farther away from the Z axis. Only a few hydrogen atoms in the residues are near R = 4.8 Å. Also, because the atoms in the residues are more distant from the channel, the dominant interactions between the ions or water molecules and GA arise from the backbone structures of GA. The carbonyl oxygens that are denoted by odd numbers are closer (about 3 Å) to the Z axis, while all the others (denoted by even numbers, including formyl

(13) Fornili, S. L.; Vercauteren, D. P.; Clementi, E. *Biochim. Biophys. Acta* **1984**, *771*, 151–164.
(14) Venkatachalam, C. M.; Urry, D. W. *J. Comput. Chem.* **1983**, *4*, 461–469.
(15) Matsuoka, O.; Clementi, E.; Yoshimine, M. *J. Chem. Phys.* **1976**, *64*, 1351–1361.
(16) Kistenmacher, H.; Popkie, H.; Clementi, E. *J. Chem. Phys.* **1973**, *59*, 5842–5848.
(17) Kim, K. S.; Clementi, E., unpublished data.
(18) (a) Sarges, R.; Witkop, B. *J. Am. Chem. Soc.* **1964**, *86*, 1862–1863; **1965**, *87*, 2011–2020, 2020–2027. (b) Sarges, R.; Witkop, B. *Biochemistry* **1965**, *4*, 2491–2494.

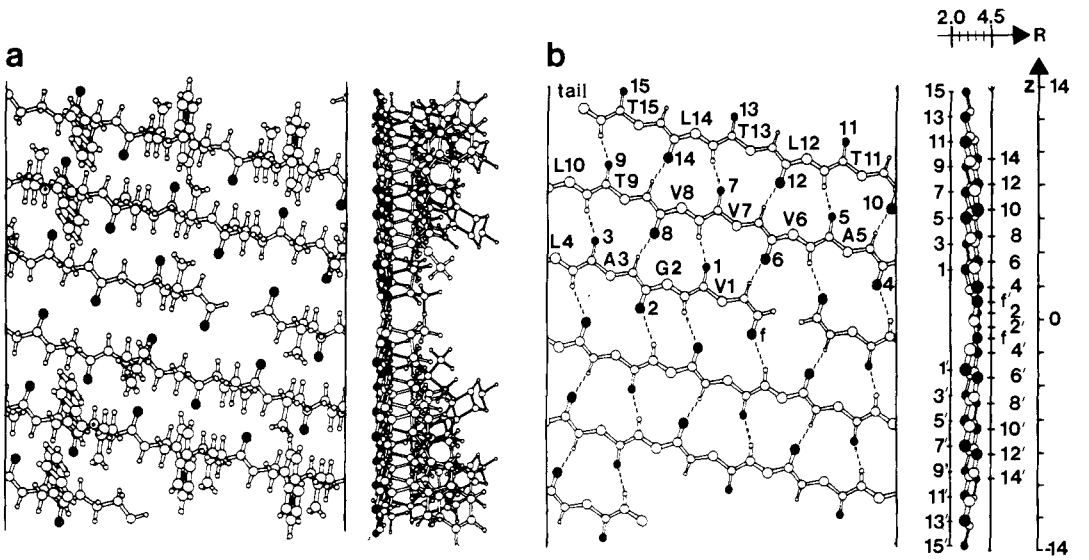

Figure 2. Cylindrical maps of GA. Inset a shows all the atoms of GA, while inset b shows only the backbone of GA. The right-most figures in each inset are R–Z projections. The R–Z projection in inset "b" includes only carbonyl atoms of the backbones. The carbonyl oxygens are darkened and numbered.

oxygens) are rather farther (about 3.7 Å) from the Z axis. Accordingly, the main contribution to the interaction energy comes from the odd-numbered carbonyl oxygens (which are nucleophilic).

Figure 2b shows that the two monomers are associated with each other (formyl end to formyl end) by means of six intermolecular hydrogen bonds (f′–H6, 4–H2′, 2′–H4, 2–H4′, 4′–H2, f–H6′), whereas each monomer is associated with itself by means of ten intramolecular hydrogen bonds (6–H1, 1–H8, 8–H3, 3–H10, 10–H5, 5–H12, 12–H7, 7–H14, 14–H9, 9–H-tail). Each α carbon connecting the residue has a hydrogen positioned nearly parallel to the cylindrical surface of the GA backbone (see Figure 2a). This hydrogen could have (i) a hydrogen bond with the nearest carbonyl oxygen in the next strip of the cylindrical backbone chain and (ii) a hydrogen bond with the neighboring carbonyl oxygen which is in parallel with the hydrogen on the same strip. However, because the amide hydrogen is more nucleophilic, the bonding between an amide hydrogen and a carbonyl oxygen is much stronger than both of these cases (namely, the bondings between a methyl hydrogen and a carbonyl oxygen). Also, note that the distance between the hydrogen and oxygen for the amide bonding case is the shortest. Therefore, we did not draw the weak bondings for the latter cases in Figure 2b.

An important feature illustrated in Figure 2b is that the carbonyl oxygens 11, 13, and 15 (and amide hydrogens H11′, H13′, and H15′) are not hydrogen bonded. This suggests that these three carbonyl oxygens can undergo relatively large librations compared with other carbonyl oxygens. This libration will lead to stronger interaction energy between cation and GA, unless those oxygens are strongly associated with neighboring phospholipids.

Based on this prerequisite structural understanding of GA, we can advance to the study of the interaction energetics of ions with GA. The previously reported interaction energies of potassium,[11] sodium,[12] and water[13] with GA, can be used to estimate the difference between K^+ and Na^+ selectivities of the ion channel. The first column (GA) of Figure 3 aids a systematic analysis by showing the X–Y projections of eight subvolumes of the GA channel. Each subvolume includes the atoms of GA which are between $X = \pm 6$ Å (abscissa) and $Y = \pm 6$ Å (ordinate) and between $Z - 3$ Å and $Z + 3$ Å for the given plane (Z = 0, 2, 4, ..., 14 Å). The $Z = 0$ plane intersects the GA dimer at its midpoint. In the second, third, and fourth columns of Figure 3 are the isoenergy maps (X–Y cross sections for each Z value) for the channel interacting with H_2C, K^+, and Na^+, respectively. The area of each map has the area between $X = \pm 6$ au and $Y = \pm 6$ au. Note that the length scale used for the maps has been expanded by a factor of about 2 over the scale used for the GA subvolumes. A spiraling arrow at the center of each inset in the first column (GA) of Figure 3 shows (i) where a helical atomic chain begins (the bottom of the segment is indicated by the tail of the arrow), (ii) the midpoint (shown by a cross), and (iii) where the helical chain ends (the top of the segment is denoted by the head of the arrow). Each inset also shows which carbonyl oxygens or residues are near the corresponding Z plane. If the carbonyl oxygens are closer to the center of the channel cross section (i.e., odd numbers), they are indicated with larger letters for emphasis, because they make dominant contributions to the interaction energy in that plane. Note that Val, Gly, Ala, Leu, and Trp are abbreviated by V, G, A, L, and T, respectively. For each isoenergy map in the second, third, and fourth columns of Figure 3, the minimum interaction energy is shown in the inset in units of kilocalories/mole.

The top inset of Figure 4 depicts the minimum interaction energies given as functions of R for H_2O, K^+, or Na^+ in the channel. The lower insets show the X–Z projections of the isoenergy maps for GA with H_2O, K^+, and Na^+ alongside the corresponding projection of the GA backbone. Figure 5 plots the corresponding cylindrical isoenergy maps for R = 2.0 and 2.5 au.

The cross sections of the channel shown in Figure 3 are not circular but have irregular shapes, with a conspicuous long earlobe, which gradually evolve and change along Z. As Z increases, the long earlobe turns around clockwise in the same direction as the helical turns of atoms of the GA channel. In particular, for the cases of Z = 4, 6, 8, 10, and 12 Å, the earlobe is across the channel from the midpoint of the arrow (indicated by a cross). That is, it is opposite to the atoms of the helical chain on a given Z value. For a given value of Z, there is a low-energy region across the channel from the helical chain, which corresponds roughly to the space in between the turns of the chain. This low-energy well also traces out a helical path, and the small size of the channel forces the water and cations into the helical energy well. Thus, the cations and water molecules move along helical paths as they traverse the channel. These arguments are born out in the lower four insets of Figure 4, wherein the earlobes for H_2O/GA, K^+/GA, and Na^+/GA turn around helically along the Z axis because they are positioned between the helical GA backbone atom layers.

Examination of the cases $Z = 0$ and 2 Å shows that there are two earlobes. One is opposite to the midpoint of the helical chain, as described above, while the other is at the junction of the A and B monomers. The alignment of this particular earlobe (in the X–Z plane) does not change with Z; in this region, there are fewer backbone than elsewhere along the Z axis. For the case $Z = 2$ Å, the low-energy well for the cations is on the same side of this channel as the chain, i.e., the low-energy well is opposite to the earlobe across the channel. However, this exception can be at-

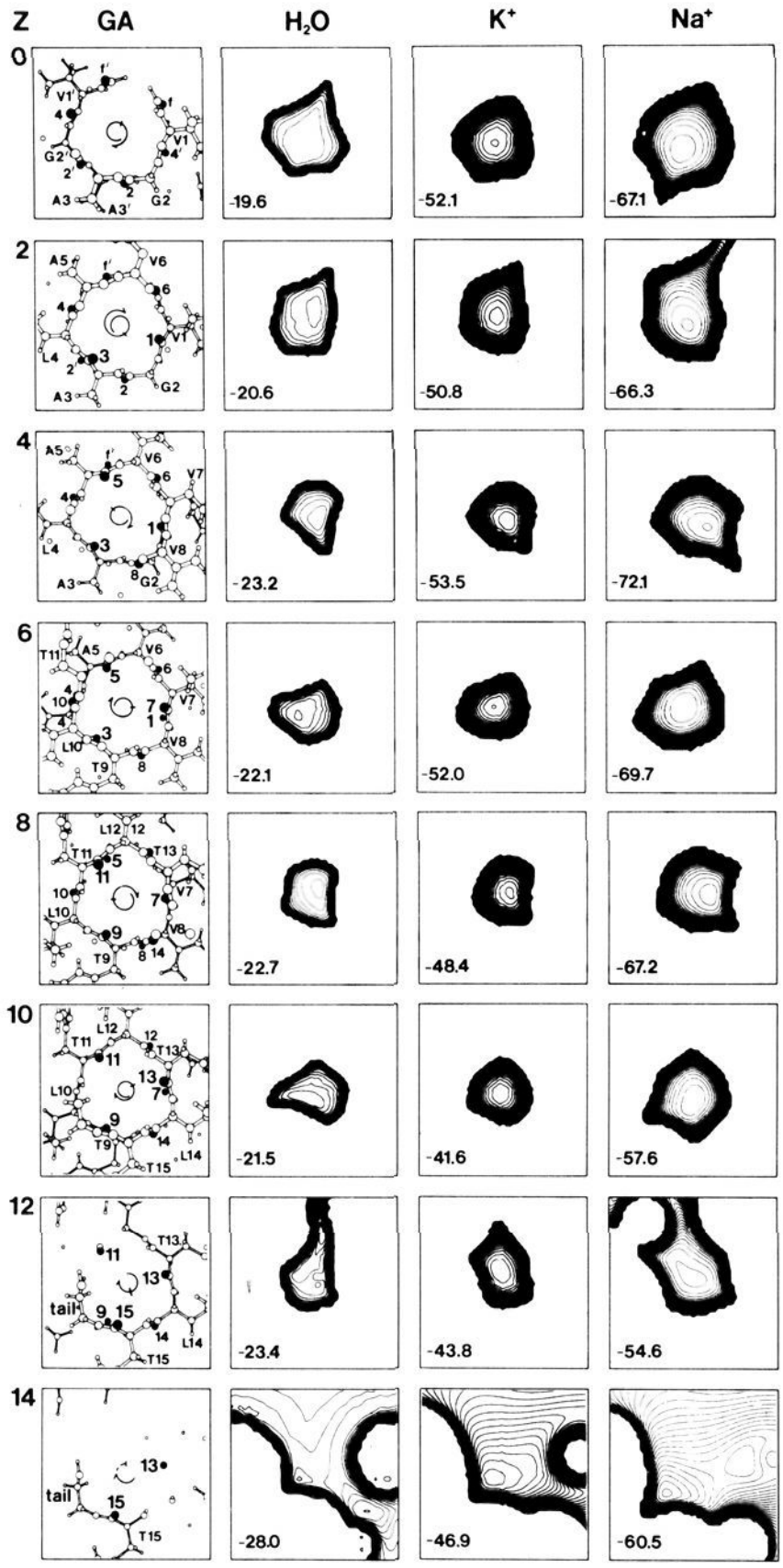

Figure 3. Isoenergy maps in X–Y projections for Z = 0, 2, 4, 6, ..., 14 Å along the Z axis. At the top-left corner of each row is the Z coordinate in angstroms. In the first column are the subvolumes of GA which are in the range between $Z - 3$ Å and $Z + 3$ Å for the given Z coordinate. On the second, third, and fourth columns are the isoenergy maps for H_2O, K^+, and Na^+ interacting with GA, respectively. The minimum energy value in each map is inserted in units of kilocalories/mole. The insets in the first column cover the area between $X = \pm 6$ Å and $Y = \pm 6$ Å, while the remaining figures in the second, third, and fourth columns cover the area between $X = \pm 6$ au and $Y = \pm 6$ au. See text for the notation in the GA column.

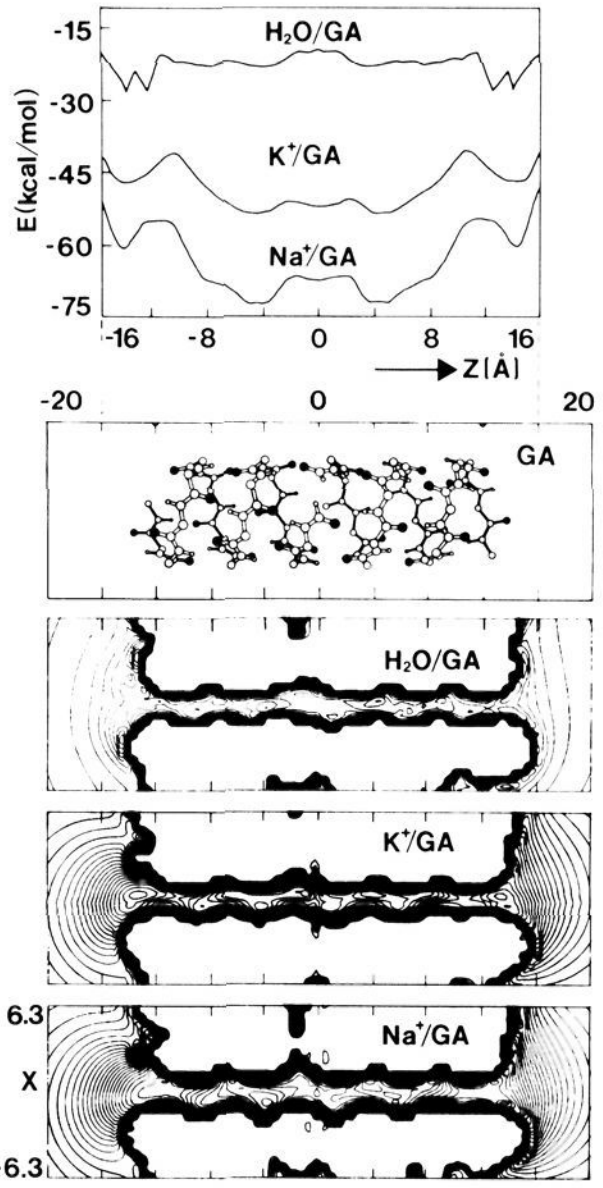

Figure 4. Minimum interaction energies of H_2O, K^+, and Na^+ with GA inside the channel as function of Z (top), and the isoenergy maps for H_2O, K^+, and Na^+ in the X–Z projection, for comparison with the energy profiles and the backbone of GA along the Z axis. (The carbonyl oxygens of GA are darkened.)

tributed to the presence of the carbonyl oxygens 1, 2, 3, and 6 (cf. Figures 2 and 3). Oxygens 1 and 3 in GA begin the spiral of inner carbonyl oxygens that follows the backbone and as such, they have an unsymmetric effect on the channel potential. For the subvolumes at $Z = 0$ Å, there are no carbonyl oxygens inside the channel.

For Z = 4–12 Å the inner carbonyl oxygens are more or less evenly distributed around the channel because two nearly superposed carbonyl oxygens in the same location in each inset are not in the same plane but lie above and below the Z plane. Nevertheless, a Na^+ ion (which has a small van der Waals radius) tends to be closer to the nearest carbonyl oxygen, because the interaction energy between Na^+ and carbonyl oxygen has a very deep potential well at a distance of 2.1–2.2 Å. Such a tendency is rather weak for a K^+ ion (which has the deep potential well at a distance of 2.5–2.6 Å), because the odd-numbered carbonyl oxygen is only at a distance of 2.9–3.0 Å from the cylindrical axis. Thus, it is expected that for Cs^+, the contribution of the carbonyl oxygens to the interaction energy would be almost uniformly distributed around the channel.

Figure 2b shows that the carbonyl oxygens are in between two neighboring strips of the GA helical chain but a little toward the strip to which oxygens are attached; so is the ion. On the other hand, the atoms in the chain exhibit a repulsive short-range force against the ion; thus, the ion is also in between two strips of the chain. These two factors (the deep interaction well due to carbonyl oxygen and the steeply changing short-range repulsive interaction due to the atoms in the chain) combine to help determine the most energetically favorable ion path in the channel. In either way, the ion path lies inbetween the two strips of the chain. Therefore, the paths taken by the cations inside the channel will be like those shown in Figure 6. The paths for cations near $Z = 0$ Å are not shown because in this region the paths are expected to be more complicated, as discussed above.

Figures 3, 4, and 5 enable another comparison between K^+ and Na^+. In the figures, the cross section of Na^+ is much larger than that of K^+. In Figures 3 and 4, the cross section (excluding the hard-core region) of K^+ has a radius of about 2 au, while that of Na^+ has a radius of about 3 au. If only the energetically favorable region is considered, the radii of the cross sections (within the dark boundary) of K^+ and Na^+ are about 1.4 and 2 au, respectively. In the cylindrical isoenergy maps of Figure 5, the hard-core regions are not conspicuous for $R = 2.0$ au but become so for $R = 2.5$ au. In particular, for K^+ at $R = 2.5$ au, the hard-core region is so dominant that no K^+ ion can move through the channel along such a cylindrical surface. For Na^+ at R =

Table I. Bonding Structures of Cations and Nine Water Molecules (See Text for Details) (Units of Coordinate and Distance Are in angstroms and Others Are the Carbonyl Oxygen Numbering of GA)

K^+ or Na^+	Z	R	0/no.	0/dist	0	1	2	3	4	5	6	7	8	9
						A. K^+								
a	−0.8	−0.6			9′	5′	1′	6′	⟨−⟩	4	1	3	7	9
b	2.7	0.4	1	2.91	9′	12′7′5′	3′	1′	4′	2′	⟨1⟩	3	7	9
c	6.1	0.5	5	2.78	9′	12′7′5′	3′	1′	2	4	1	⟨5⟩	7	11
d	7.9	0.5	7	2.69	9′	7′5′	3′	1′	4′	2′	1	3	⟨7⟩	9
e	11.4	0.5	11	2.72	9′	12′7′5′	3′	1′	4′	4	1	3 5	7	⟨11⟩
f	15.0	0.7	15	2.64	9′	7′5′	3′1′	4′f		1	3	7	9	⟨15⟩
						B. Na^+								
a	−0.1	0.9	2′	2.89	9′7′	5′	1′	4′f	⟨2′2⟩	f′4	1	5	7	
b	3.5	0.8	1	2.28	9′	12′7′5′	3′	1′	2	f′	⟨1⟩	3	7	9
c	6.0	0.7	5	2.79	9′	7′5′	3′1′	f	2′	f′	1	⟨3 5⟩	7	9
d	8.7	0.8	7	2.50	9′	12′7′5′	3′	1′	2	f′4	1	5	⟨7⟩	11
e	11.8	1.1	11	2.23	9′	7′5′	3′1′	f	2′2	f′	1	5	9	⟨11⟩
f	15.4	0.6			9′	7′5′	3′1′	f	2′	1	3	7	9	

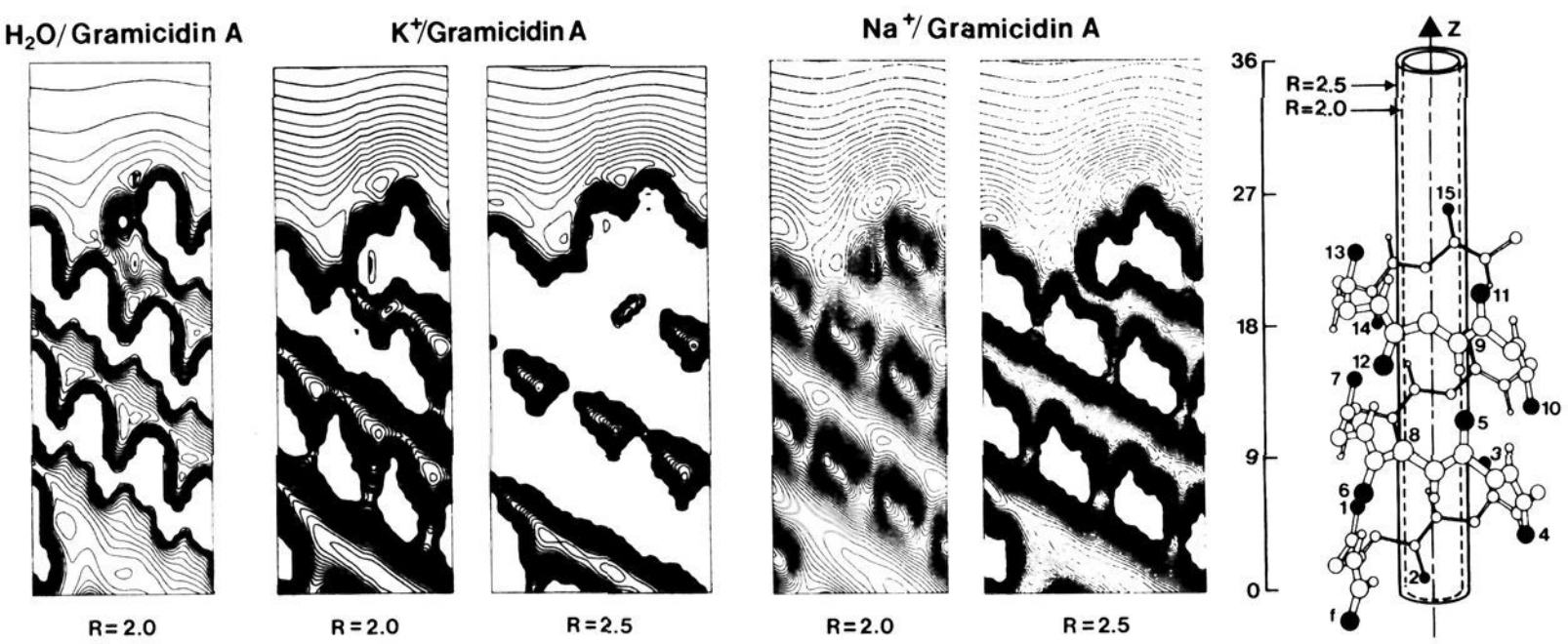

Figure 5. Cylindrical isoenergy maps shown in the Z–$R0$ projection with fixed radii R = 2.0 and 2.5 au for the interaction energies of H_2O, K^+, and Na^+ with GA. Z coordinates are given in atomic units. The right-most inset is a representation of the helical GA backbone only.

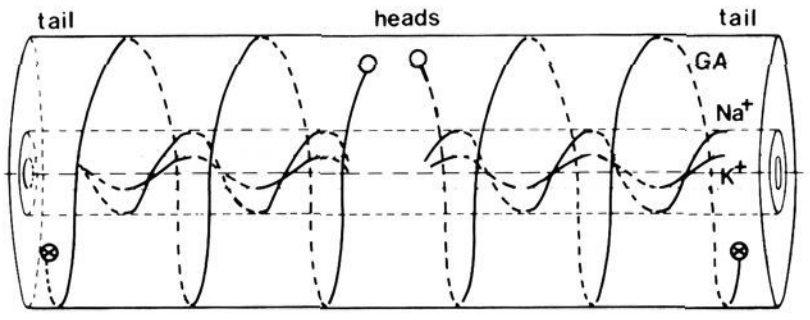

Figure 6. Schematic representation of helical paths of K^+ and Na^+ inside the GA channel. The helical pattern of the GA backbone is also sketched.

2.0 au, however, the hard-core region does not appear yet; thus, if otherwise energetically favorable conditions are given, a Na^+ ion may move through the channel along this cylindrical surface. Overall, the cylindrical maps show similar patterns for H_2O at R = 2.0 au, K^+ at R = 2.0 au, and Na^+ at R = 2.5 au. Also, it can be seen from Figure 3 that the minima in the cross sections for Na^+ trace out more helical paths, while those for K^+ are more linear along the Z axis. However, it should be noted that these results were obtained from a rigid GA model. If carbonyl librations are seriously considered, the helical paths still lie in between the two neighboring backbone strips but a little more toward the strip, the carbonyl of which is attached toward the other strip.

Finally, we notice that the interaction energy for Na^+/GA is larger than that for K^+/GA, (i) partly because Na^+ has stronger interaction energies with the GA atoms and (ii) partly because Na^+ can more readily find the energetically favorable positions in GA (that is, along the R direction), while K^+ cannot easily move away from the Z axis. It follows that the interaction energy surface of Na^+/GA is less smooth than that of K^+/GA.

III. Structural Features of Cations and Water Molecules with GA

Since preliminary MC simulations (performed at 300 K) were previously[8,9] reported, we describe here a detailed analysis which shows how the water molecules and cations interact with the carbonyl oxygens of GA and also report results for the solvation and hydration energetics.

The bonding structures of water molecules in the GA channel in the presence of a K^+ ion are shown in Figure 7. In the top insets, only the carbonyl groups of the backbone are shown. The other insets (a–f) show how bonding structures of the ion and the *neighboring water molecules change with the position of the ion* along the Z axis. The average positions of the K^+ ion are at (a) Z = −0.8, (b) Z = 2.7, (c) Z = 6.1, (d) Z = 7.9, (e) Z = 11.4, and (f) Z = 15.0 Å. The insets in the left column are X–Z projections, while those on the right are Y–Z projections. In the top insets, the carbonyl oxygens are darkened and numbered according to the scheme in Figure 2, while in the remaining insets *nine water molecules inside the channel* and one ion are darkened (instead of the carbonyl oxygens) in order to show the hydration structures. Also, the ions are circled, and the hydrated carbonyl oxygens are indicated by their corresponding numbers.

The bonding structures of a GA channel in the presence of a Na^+ ion are shown in Figure 8. The GA backbone atoms for the channel are shown in the top insets. Other aspects of Figure 8 are the same as those of Figure 7, except that the average positions of the Na^+ ion are located at (a) Z = −0.1, (b) Z = 3.5, (c) Z = 6.0, (d) Z = 8.7, (e) Z = 11.8, and (f) Z = 15.4 Å.

Table I lists the carbonyl oxygens which are hydrogen bonded to the nine water molecules and the ion (K^+ or Na^+) in the channel. Also given are the following: (i) Z, the average value of the Z coordinate of a cation in the channel; (ii) R, the average

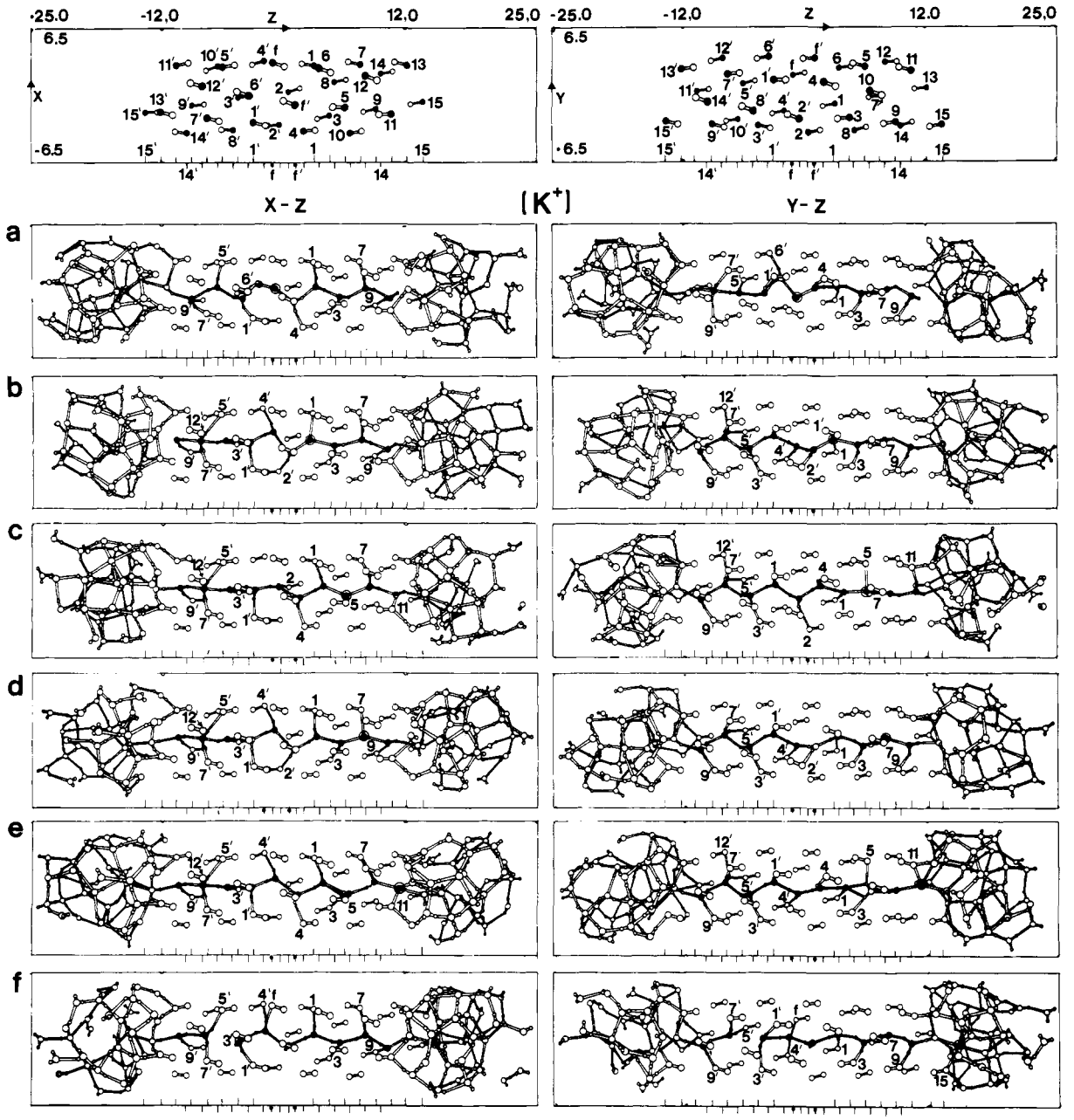

Figure 7. Bonding structural features in the solvated GA channel in the presence of a K^+ ion. In the top insets only, the carbonyl groups are shown for the GA channel. In the remaining insets, the average positions of the K^+ ion are (a) $Z = -0.8$, (b) $Z = 2.7$, (c) $Z = 6.1$, (d) $Z = 7.9$, (e) $Z = 11.4$, and (f) $Z = 15.0$ Å.

distance from the Z axis to the cation; (iii) O/no., the number of the nearest GA carbonyl oxygen bound to the cation; (iv) O/dist, the distance from the cation to the nearest carbonyl oxygen (O/no.); and (v) 0–9, the numbers of the GA carbonyl oxygen that are bound to each of the nine water molecules and to the cation in the channel. The water molecules and the ion are numbered 0–9 from left to right without distinguishing the cation from the water molecules, and the carbonyl oxygens are labeled as in Figure 2. The cation position is shown in brackets in the table to distinguish it from the water molecules and to show qualitatively how the cation is surrounded by water molecules. For example, in the case of water molecules, the 0's are positioned around $Z = -11$ Å, and the 9's are positioned around $Z = 11$ Å. In the case of "f", the cation is placed just outside the channel.

Table I in conjunction with Figures 7 and 8 shows that most of the water molecules strongly hydrate the odd-numbered oxygens, while a few water molecules weakly hydrate even-numbered oxygens. This occurs because the odd-numbered oxygens are generally closer to the water molecules. The most important feature to be observed is the following: inside the channel, *the average radial position (R) is 0.5 ± 0.1 Å for a K^+ ion, while it is 0.8 ± 0.2 Å for a Na^+ ion.* This suggests that the Na^+ ion describes a larger helix than the K^+ ion, as found in the previous section. Table I also shows that both cations have larger R values near $Z = 0$ Å than for other Z values.

As reported previously,[11,12] there are nine water molecules inside the channel (i.e., between −12 and 12 Å) for both cations; there is no significant difference between Na^+ and K^+. Compared with the osmotic and diffusional experimental value[19] (6–7 water molecules) and also with electrokinetic experimental values (6–7 water molecules by Rosenberg[20] and 12 water molecules by Levitt[21]), our theoretical value is thus intermediate between the two extremes. However, the correct number will depend on the medium (phospholipids, bulk water, etc.) at the two outlets and also on the GA structural changes.

(19) Rosenberg, P. A.; Finkelstein, A. *J. Gen. Physiol.* **1978**, *72*, 327–340.
(20) Rosenberg, P. A.; Finkelstein, A. *J. Gen. Physiol.* **1978**, *72*, 341–350.
(21) Levitt, D. G.; Elias, S. R.; Hautman, J. M. *Biochim. Biophys. Acta* **1978**, *512*, 436–451.

Table II. Coordination Numbers (W1, W2). Average Coordinating Distances (WD1, WD2 in Å) and Solvation Energies (S1, S2) of the First and Second Solvation Shells for Cation–Water–GA Systems, and Their Energy Sum (S12), Energy Components Contributed from Cation (I/W, I/GA, I/T), and Standard Deviation of Cation Positions (STD in Å) (Units of Energy Are in kJ/mol. The Notation of a Through f Has the Same Meaning as in Table I)

K^+ or Na^+	W1	W2	WD1	WD2	S1	S2	S12	I/W	I/GA	I/T	tot	tot/No.	STD
						A. K^+							
a	2	2	2.48	3.77	−130	−77	−207	−302	−210	−361	−6624	−81.8	0.23
b	2	2	2.52	4.45	−134	−62	−196	−278	−209	−347	−6648	−82.1	0.28
c	2	2	2.48	4.76	−138	−48	−186	−288	−210	−354	−6651	−82.1	0.27
d	2	3	2.50	5.06	−136	−52	−190	−292	−197	−342	−6631	−81.9	0.29
e	3	7	2.62	*a*	−184	−84	−268	−396	−169	−367	−6658	−82.2	0.28
f	5	*a*	2.72	*a*	−278	*a*	*a*	−522	−187	−448	−6742	−83.2	0.35
						B. Na^+							
a	2	2	2.07	3.81	−187	−76	−263	−414	−278	−485	−6835	−84.4	0.38
b	2	2	2.10	4.17	−188	−66	−254	−400	−294	−494	−6854	−84.6	0.27
c	2	2	2.10	4.17	−188	−42	−230	−402	−287	−488	−6863	−84.7	0.35
d	2	3	2.11	4.66	−188	−84	−262	−460	−270	−500	−6855	−84.6	0.30
e	4	7	2.37	*a*	−318	−90	−408	−710	−217	−522	−6886	−85.0	0.30
f	6	*	2.34	*a*	−443	*a*	*a*	−776	−165	−553	−6953	−85.8	0.43

[a] Uncertain values.

Table III. Solvation Energy (Units in kJ/mol; See the Notation of Table I for a and f. The a/s and f/s Denote Accumulated Sums. S × No. Denotes Solvation Energy of the Numbered Shell. ST Denotes Total Solvation Energy)

K^+	S1	S2	S3	S4	S5	ST	Na^+	S1	S2	S3	S4	S5	ST
a	−130	−77	−28	−8	+0		a	−187	−76	−34	−8	−4	
a/s	−130	−207	−235	−243	−243	−302	a/s	−187	−263	−297	−305	−309	−414
f/s	−271					−522	f/s	−443					−776

Next, the solvation and hydration energetics are examined. Table II gives (i) the number of water molecules solvating the ion in the first (W1) and second (W2) shells, (ii) the average distance from the ion to the water molecules of the first (WD1) and second (WD2) shells, (iii) the total solvation energy contribution from the first (S1) and second (S2) shells, the sum (S12) of S1 and S2 and total solvation energy (I/W), (iv) the interaction energy of the ion with GA (I/GA), (v) the total ion interaction energy (I/T), (vi) the total energy of the system (tot) and total energy of the system per mole of water (tot/no.), and (vii) the standard deviation of the ion coordinate (STD). We note here that the total energy of the system (tot) is partitioned into components due to the cations (I/T) and to the water (W/T) defined as follows: tot = I/T + W/T, where I/T = $^1/_2$(I/W) + I/GA, W/T = W/W + $^1/_2$(W/I) + W/GA, and I/W = W/I.

Since the water molecules inside the channel form a chainlike strand, the cations in the channel are hydrated by two water molecules in each solvating "shell". As cations approach the mouth of the channel, they are solvated by more than two water molecules. For example, when the K^+ ion is at about Z = 7.9 Å (see row d in Table IIA), the second solvation shell of the cation contains three water molecules. When the K^+ ion is at about Z = 11.4 Å (cf. row e), the first solvation shell contains three and the second shell contains seven water molecules. Thus, it follows from Table II that when a K^+ ion is inside the channel, the solvation energies of the first and second shell and also the total for all the shells are about −130, −60, and −290 kJ/mol, respectively, while when Na^+ is inside the channel they are about −190, −60, and −400 kJ/mol, respectively. Inside the channel, it is also found that the average distance from an ion to the first shell water molecules is 2.5 Å for K^+ and 2.1 Å for Na^+. However, outside the channel, particularly for the f case, the distance is more than 2.7 Å for K^+ and more than 2.3 Å for Na^+.

The f cases in Tables II and III for Na^+ also show that the Na^+ ion is solvated by six water molecules in the first solvation shell, with the solvation energy contribution (S1) of −443 kJ/mol, while the total solvation energy (ST) is −776 kJ/mol. This can be compared with bulk water. For the latter case, the solvation energy contribution from the first shell (containing six water molecules) is reported by Chandrasekhar et al.[22] to be −714 kJ/mol, and the total solvation energy is −1170 kJ/mol. These theoretical solvation energies are too large due to the neglect of the quantum effects, polarization effects, and many body effects. The neglect of the quantum effects is particularly responsible for the overestimation of the solvation energies by the water molecules in the first solvation shell; the neglect of the polarization is responsible for the overestimation of the interaction energies between an ion and water dipoles at large separation, due to the neglect of screening effects. In our case, these effects should be similar, so that our solvation energy from the first solvation shell is definitely overestimated. Since the dielectric constant is much smaller in linear chainlike water (ϵ is about 5–6)[23] than in bulk water (ϵ is about 80), the polarization effects are smaller. Therefore, the solvation energies by second, third, and fourth solvation shells are expected to be more reliable. Our results for these solvation energies (−77, −28, and −8 kJ/mol for K^+ and −76, −34, and −8 kJ/mol for Na^+, respectively) can be compared with those of Wilson et al.[9] (−94, −77, and −60 kJ/mol for K^+ and −104, −77, and −65 kJ/mol for Na^+, respectively). These results clearly show the effect of including the water molecules outside of the channel; the contribution of the solvation energies from the higher solvation shells decreases rapidly in our model.

Comparing our result with the theoretically computed solvation energies for bulk water, we find that the case f is showing bulklike behavior, an observation that is also supported by the average distance (WD1) from a cation to the water molecules in the first solvation shell, 2.34 Å. This is in the range of the average distance for the bulk case which is 2.3–2.4 Å.[24] On the other hand, for

(22) Chandrasekhar, J.; Spellmeyer, D. C.; Jorgensen, W. L. *J. Am. Chem. Soc.* **1984**, *106*, 903–910.

(23) Urry, D. W.; Alonso-Romanowski, S.; Venkatachalam, C. M.; Trapane, T.; Harris, R. D.; Prasad, K. U. *Biochim. Biophys. Acta* **1984**, *775*, 115–119.

(24) (a) For theoretical data, see for example: Kistenmacher, H.; Popkie, H.; Clementi, E. *J. Chem. Phys.* **1974**, *61*, 799; **1973**, *59*, 5842; **1973**, *58*, 1689, 5627. Clementi, E.; Barsotti, R. *Chem. Phys. Lett.* **1980**, *59*, 21. Reference 8: Mezei, M.; Beveridge, D. L. *J. Chem. Phys.* **1981**, *74*, 6902. Impey, R. W.; Madden, P. A.; McDonald, I. R. *Mol. Phys.*, in press. Heinzinger, K.; Vogel, P. C. *Z. Naturforsch., A* **1976**, *31*, 463. Szase, G. I.; Heinzinger, K. *Z. Naturforsch., A* **1979**, *34*, 840. (b) For X-ray data, see for example: Neilson, G. W.; Enderby, J. E. *Annu. Rep. Progr. Chem. Sect. C* **1979**, *76*, 185. Enderby, J. E.; Neilson, G. W. *Rep. Progr. Phys.* **1981**, *44*, 38. Franks, F., Ed. "Water: A Comprehensive Treatise"; Plenum Press: New York, 1979; Vol. 6, Chapter 1. (c) For neutron diffraction data, see for example: Newsome, J. R.; Neilson, G. W.; Enderby, J. E. *J. Phys. C* **1980**, *13*, L923. Cummings, S.; Enderby, J. E.; Neilson, G. W.; Newsome, J. R.; Howe, R. A.; Howells, W. S.; Soper, A. K. *Nature (London)* **1980**, *287*, 714. (d) For solvation energy, see for example: Franks, F., Ed. "Water: A Comprehensive Treatise"; Plenum Press: New York, 1979; Vol. 3, Chapter 1.

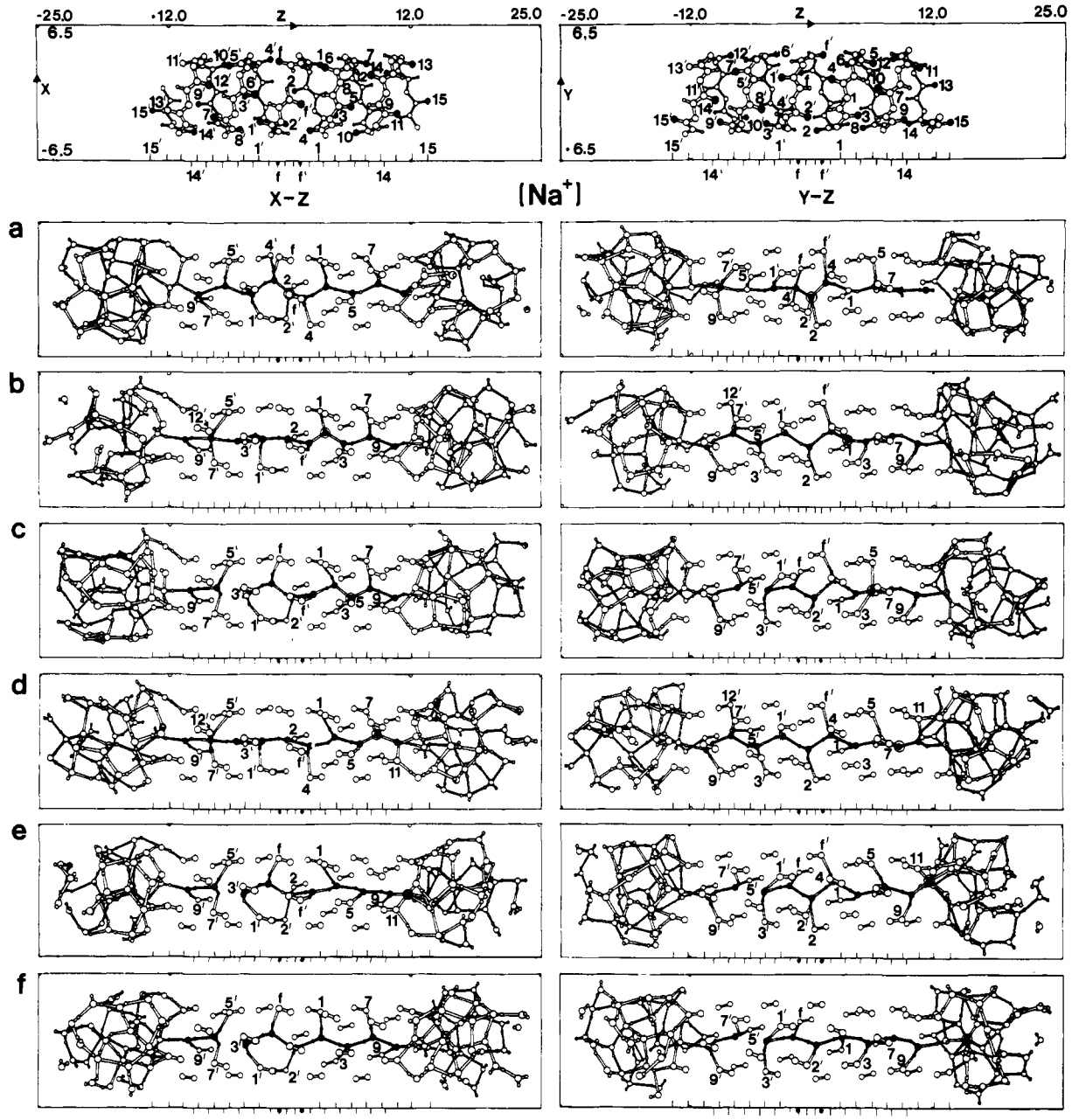

Figure 8. Bonding structural features in the solvated GA channel in the presence of a Na^+ ion. In the top insets only, the GA backbones are shown for the GA channel. In the remaining insets, the average positions of the Na^+ ion are (a) Z = 0.1, (b) Z = 3.5, (c) Z = 6.0, (d) Z = 8.7, (e) Z = 11.8, and (f) Z = 15.4 Å. Compare with Figure 7 and see text for details.

the a case of Na^+, we see that Na^+ is solvated by two water molecules in each solvation shell up to the fifth shell. Inside the channel, water molecules form a linear chain. If Na^+ is near the center of the channel, water molecules tend to line up toward the ion up to five water molecules from both left and right sides of the ion, respectively. This can be compared with the bulk system in which only up to the second solvation shell shows such tendency. Our quasi-linear and quasi-bulk systems can be compared with the real bulk system which has been extensively studied.[24]

In case f for K^+, K^+ is solvated by five water molecules in the first solvation shell with the solvation energy contribution of −271 kJ/mol, while the total solvation energy is −522 kJ/mol. Here, the K^+ ion is bonded by carbonyl oxygen 15 of GA. Therefore, for the bulk case, K^+ will tend to be solvated by six water molecules in the first solvation shell, as in the Na^+ case. Similarly to the a case in Table III, K^+ is solvated by two water molecules in each solvation shell up to the fourth shell. For this reason, the capacity of solvation for K^+ is somewhat smaller than that for Na^+. Also we notice from Table II that Na^+ is generally better solvated than K^+, because Na^+ has a smaller van der Waals radius.

Previously in this report, the interaction energies of ions (I = K^+ or Na^+) with water (I/W) and GA (I/GA) and the total ion interaction energy (I/T) were discussed. Figure 9a compares these values for both cations. Note that the dotted curves in the figure (shown with parentheses for I/GA) are taken from the top inset of Figure 4 (which are obtained without thermal effects for the interaction of a single ion with anhydrated GA).

Table IV lists the interaction energies of the nine water molecules (W9) in the channel with ion (W9/I), with GA (W9/GA), and with water (W9/W:W represents all water molecules, that is, 81 molecules) and these sums (W9/T). From these data we find that the nine water molecules interact more strongly with GA compared with that with water or an ion. This fact, combined with the very small cross sections of the channel (as discussed earlier), suggests that an ion will push a column of water ahead of it in order to pass through the channel. This may be related with the recent experimental indication[24] that the dominant factor to control the rate of ion transport through the channel would be the entrance–exit barrier height rather than the diffusional path length of the ion in the channel.

Table IV. Energy Components for W9/K^+ and W9/Na^+ (Units Are kJ/mol; See Table I for Notation a–f for K^+ and Na^+)

K^+	W9/I	W9/W	W9/GA	W9/T	Na^+	W9/I	W9/W	W9/GA	W9/T
a	−123	−114	−694	−931	a	−153	−116	−700	−970
b	−111	−131	−720	−962	b	−145	−133	−721	−998
c	−104	−142	−715	−960	c	−140	−138	−712	−990
d	−94	−150	−718	−962	d	−129	−149	−716	−994
e	−61	−166	−735	−962	e	−80	−162	−730	−972
f	−28	−180	−752	−959	f	−31	−183	−750	−964

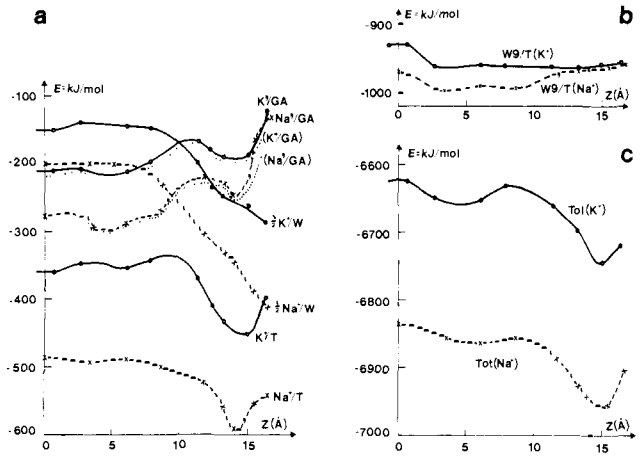

Figure 9. Energy profiles obtained by MC simulations for K^+ and Na^+ cations interacting with the solvated GA. Inset a shows the interaction energy components contributed from cations. Inset b shows the total interaction energy components contributed from the nine water molecules inside the channel. Inset c shows the total energies of the K^+ and Na^+ systems. See Tables II and IV and text for the notation and details.

Figure 9b charts the total interaction energies of the nine water molecules inside the channel (W9/T). Also shown in Figure 9c is the total energy of the system (tot), as listed in Table II. Figure 9a indicates that I/GA is stronger inside the channel, while I/W is stronger outside the channel because there is more water outside. However, the difference of I/W between inside and outside is greater than that of I/GA, unless Z is greater than Z = 15 Å where the value of I/GA suddenly increases. Therefore, for both cations, I/T has the minimum values near Z = 15 Å.

On the other hand, Figure 9b shows that W9/T does not significantly change with respect to the change of Z, especially for the K^+ case. Thus, in Table IV, we observe the following: as Z increases, W9/I decreases because the ion is farther from the water molecules in the channel; W9/W and W/GA increase because of the lack of hindrance for the W9/W and W9/GA interactions by the strong W9/I interactions. Also, W9/W increases partly because there is more water outside the channel. The above three contributions are mostly canceled, and thus, W9/T is almost constant along the Z axis. Therefore, the total energy of the system should depend on I/T and on the total contribution from the water molecules which are outside the channel. If the ion is inside the channel, the water molecules outside the channel would have strong water–water interaction energy. On the other hand, if the ion is outside the channel, the water molecules outside would have strong ion–water interaction energy by sacrificing the water–water interaction energy; these two energy contributions tend to be conserved. Therefore, the I/T contribution is the key term for the total energy of the system (tot). This makes the graphic shape of I/T somewhat similar to that of tot in Figure 9c, which shows, for both cations, that the minimum is near Z = 15 Å and the maximum is Z = 0 Å. It also shows that the energy difference between the maximum and the minimum is about 120 kJ/mol.

IV. Discussion and Concluding Remarks

The previous sections described that for both K^+ and Na^+, nine water molecules inside the channel are between Z = −12 and 12 Å in a linear chainlike conformation. The channel is very narrow so that only one cation or one water molecule can pass a given cross section at one time; a cation can move through the channel only by pushing over all the water molecules inside the channel. Especially for $6 < |Z| < 11$ Å, the radius of the cross section within the energetically accessible region is about 0.7 au for both H_2O and K^+ and 1.0 au for Na^+. The earlobe or deep minimum of the isoenergy map tends to lie between the helical GA backbone atomic chains. Combining these trends with the MC simulation results indicates that the cations and water molecules move along helical paths between two chains of GA backbone atoms, with off-axis radii of 0.5 ± 0.1 Å for K^+ and of 0.8 ± 0.2 Å for Na^+. In order to pass through the channel, the Na^+ ion needs a longer path (about 1.4 times) than the K^+ ion. This is consistent with the results of Wilson et al.[9] However, it should be noted, as mentioned in section III, that recent experimental data indicate that ion selectivity depends on the entrance–exit barrier at the mouth of the channel rather than the path length of the ion inside the channel. One should also notice that the classical fluid theory does not work for this GA model because the larger (energetically favorable) cross section for Na^+ does not help Na^+ to pass through the channel faster.

Some special considerations can be given to the region near the center of the channel in which the A and B monomers are joined to each other. In this region, there are fewer backbone atoms, so that the cross section is somewhat larger. Therefore, the water molecules and ion have more freedom to move around.

In section III, we have shown the bonding structures and the solvation and hydration energetics for both cations. We have also shown that for both cations, the graphs of the total internal energy of the system have similar shapes; for both cations, the difference between the maximum and the minimum for the total *internal energy* of the system is about 120 kJ/mol and the maximum and minimum are located at Z = 0 Å and near Z = ±15 Å, respectively. On the other hand, experimental data[2,25,26] show, for both cations, that the *free energy* activation barrier is 20–30 kJ/mol, the *free energy* difference between the maximum and the minimum is 30–40 kJ/mol, and there is one maximum at Z = 0 Å and two minima (one near Z = ±11 Å, and the other possibly outside the channel). The first minimum position is called a binding site. Since our calculation did not show this binding site, we think that this might come from carbonyl librations. If the three comparatively freely movable carbonyls (11, 13, and 15) and the hydroxyl oxygen of the tail part clamp the ion as discussed in section II, our simple estimation supports the possibility of such a binding site. Since the constraint of a rigid GA brings about a somewhat incorrect choice of the "GA, water, ion" geometry, it is expected that relaxation in the GA geometry will lower the total energy difference.

In order to properly compare our theoretical results with the experimental results, we must consider how the Gibbs free energy G will behave in our theoretical model. We are interested in the activation barrier and the location of the minimum and maximum. For this study, we do not need to know the absolute magnitude of G but only the change of G (ΔG), as a function of the position of the cations along the Z axis in the channel. Given $\Delta G = \Delta E + P\Delta V - T\Delta S$ at P = 1 atm and T = 300 K, the $P\Delta V$ term would be negligible compared with ΔE, but the $T\Delta S$ term should not be assumed small. For example, consider the difference in G (ΔG) for the cases when a cation is placed inside the channel and when

(25) (a) Hladky, S. B.; Haydon, B. W. *Biochim. Biophys. Acta* **1972**, *274*, 294–312. (b) Eisenman, G.; Sandblom, J. P. *Biophys. J.* **1984**, *45*, 88–90. (c) Bambergnand, E.; Lauger, P. *Biochim. Biophys. Acta* **1974**, *367*, 127–133.

(26) Urry, D. W.; Walker, J. T.; Trapane, T. L. *J. Membr. Biol.* **1982**, *69*, 225–231.

the cation is outside the channel. For the two cases, the nine water molecules inside the channel are well ordered and will give almost the same contribution, since W9/T is almost constant (see Figure 9b). Therefore, the entropy of these molecules will be small and almost the same. The ΔS contribution from the cation will be different for the two cases, because the standard deviation of the ion coordinates (STD in Table II) shows that when the cation is outside the channel, the cation is more mobile. On the other hand, the water molecules outside the channel are less mobile due to the strong solvation with the cation than those inside the channel. Thus, the entropy contributions from the water molecules outside the channel and that from the cation have opposite signs. However, since water molecules in the first and second solvation shells are strongly bound to the cation (particularly true for our simulations, owing to the simplified model), the entropy decrease of water due to the solvation of the cation is expected to be more important. In fact, when K^+ and Na^+ are solvated, the experimental solvation energies[24] of K^+ and Na^+ are reduced by 22.2 and 32.6 kJ/mol, respectively, due to the entropy effects. In our model, the upper bound of the reduction of the solvation energies due to the entropy effect can be estimated to be less than 50 kJ/mol by considering an extreme case that all the water molecules solvating the cation were frozen. Since water-water interactions along the X and Y directions were not properly considered due to an imposed hard wall, most water molecules solvating the cation oriented toward the cation, especially when the cation was outside of the channel.

Although the total energy in the asymptotic region for Na^+ has not been calculated, the internal energy activation barrier for Na^+ may be estimated to be less than 70 kJ/mol from the energy of the MC simulation calculation near $Z = 17$ Å (Figure 9c and ref 11). The free energy activation barrier will be much smaller due to the entropy effects than the internal energy activation barrier (by more than 20 or 30 kJ/mol from the aforementioned argument). Compared with experimental free energy activation barriers of 20–30 kJ/mol,[2,25,26] our result is not far from this range, but it overestimates the barrier owing to the simplified model by the following reason: (i) the bulk water characteristics outside the channel were not properly considered and (ii) these results were obtained from a rigid GA model without including phospholipids.

In order to better model the experimental system, we must first include more water by extending the boundaries to properly treat ion solvation energetics, since the energy difference between the maximum and the minimum is very different from experiment compared to the case of the activation barrier. In other words, the solvation near the minimum was exaggerated because the second solvation shell around the cation would not have proper water-water interactions owing to the limited number of water molecules used in our MC simulations. For the explanation of the first minima, i.e., experimental binding sites, the theoretical model needs to include the libration of the carbonyl oxygens 11, 13, and 15 and the hydroxyl oxygen motion of the tail. These structural changes will possibly allow the minima near $Z = \pm 11$ Å. Also, the free energy difference between the maximum and the minimum might well be reduced by the following argument. If the theoretical model were to include the phospholipid interactions with GA, the energies near the estuary region will be less negative because the solvation energy of the cations will be reduced due to the phospholipid effect. If the model includes the dynamical motion of GA such as libration, bending, stretching, contraction, and vibration of GA, energy transfer among GA, cation and water, etc., then the energies inside the channel will be more negative. Therefore, in a real system, the maximum will be lowered and the minimum will be raised, resulting in a lowering of the energy difference, and this would be consistent toward the experimental value.

Work is now in progress attempting to introduce the intramolecular motions, increase the number of water molecules, and approximate the phospholipids effect. Since membranes very mobile, the latter is expected to be very important, but, also most difficult to quantitatively analyze either with laboratory or computer experiments. We note, finally, that this work has been performed by using a parallel supercomputer, ICAP1, described elsewhere,[27] which was essential for this type of very demanding computer experiments.

Acknowledgment. We thank the National Foundation for Cancer Research (NFCR) for financial support. We also thank Dr. M. C. Wojcik, Dr. J. Ball, and Prof. G. Lie for useful discussions and critical reviews of this manuscript.

(27) (a) Clementi, E.; Corongiu, G.; Detrich, J.; Chin, S.; Domingo, L. *Int. J. Quantum Chem. (Quantum Chem. Symp.)* **1984**, *18*, 601. (b) Clementi, E.; Corongiu, G.; Detrich, J.; Khanmohammdbaigi, H.; Chin, S.; Domingo, L.; Laaksonen, A.; Nguyen, H. L. "Parallelism in Computational Chemistry" in "Structure and Motion: Membranes, Nucleic Acids and Proteins"; Clementi, E., Corongiu, G., Sarma, M. H., Sarma, R. H., Eds.; Adenine Press: Guiderland, NY, 1985; pp 49–85.

A Stereochemical Imperative in Dehydrogenases: New Data and Criteria for Evaluating Function-Based Theories in Bioorganic Chemistry

Steven A. Benner,*[1] Krishnan P. Nambiar, and Geoffrey K. Chambers

Contribution from the Department of Chemistry, Harvard University, Cambridge, Massachusetts 02138, and The Museum of Comparative Zoology, Harvard University, Cambridge, Massachusetts 02138. *Received August 29, 1984*

Abstract: We present data that show that a pair of ethanol dehydrogenases from yeast and *Drosophila* have opposite stereoselectivities. These data support the notion that the stereoselectivity in dehydrogenases reflects a "stereochemical imperative" (Nambiar et al. *J. Am. Chem. Soc.* **1983**, *105*, 5886–5890), and further weaken "historical" arguments explaining dehydrogenase stereoselectivity as a trait conserved during the divergent evolution of modern dehydrogenases from a limited number of ancestral dehydrogenases. Finally, we note that the recent challenges (Oppenheimer, N. J. *J. Am. Chem. Soc.* **1984**, *106*, 3032–3033) to our theory explaining the stereoselectivity of alcohol dehydrogenases reflect a misstatement of our thesis and overlook most available data. Furthermore, the challenge overlooks the general requirement that the physiological role of an enzyme must be "well-defined" if data from that enyzme are to be used to test a functional theory in bioorganic chemistry.

One appropriate (but often neglected) goal of bioorganic chemistry is to distinguish between those details of enzymic catalysis that are the products of natural selection and those that are not.

0002-7863/85/1507-5513$01.50/0